

STUDY OF AEROSOL POLLUTION OF THE ATMOSPHERE OVER AN INDUSTRIAL REGION USING LIDARS

A.P. Ivanov, A.P. Chaykovskii, F.P. Osipenko, I.S. Khutko, M.M. Korol',
V.N. Shcherbakov, V.P. Kabashnikov, A.I. Bril', V.M. Popov,
A.A. Kovalev, A.M. Samusenko, and M.A. Drugachenok

*Institute of Physics, Belorussian Academy of Sciences
Institute of Radiobiology, Belorussian Academy of Sciences
"EkomirB Republic Scientific Technical Center*

Belorussian Department of Natural Resources and Environmental Protection, Minsk

Received May 6, 1997

We discuss here the methodology of using lidar stations for ecological monitoring of air over an industrial center. The city of Soligorsk, Belorussia, has been taken as an example. The lidars were used to identify the sources of dust emissions, to map the dust mass concentration, and to estimate the rate of dust sedimentation. The lidar data obtained, enabled us to estimate the rates of dust emissions coming from industrial enterprises, as a whole, and from their individual technological installations. Contributions from such distributed pollution sources as dumps, construction sites and others are evaluated. The entire bulk of thus compiled information has been used to construct a mathematical model of the aerosol pollution transport in the region under study. The input parameters to this model are the rates of dust emissions measured and meteorological quantities. Calculated values of the aerosol concentration in the near-ground layer and the rate of aerosol sedimentation have been compared with the data of observations. The model is available as a computer codes and may be used for numerically predicting the level of atmospheric pollution. The forecast may be produced with the account for different meteorological situations and varying intensity of the production process.

1. INTRODUCTION

To remediate air over industrial regions, the pollution sources in the area must be preliminarily studied, their intensity estimated, and chemical conversions and transport of the contaminating species under different meteorological conditions investigated. In the industrial regions, not only stationary, localized sources may contribute to air pollution, but also distributed, inhomogeneous and nonstationary ones. Transport of pollutants within an industrial zone is confined to the atmospheric boundary layer. Methods and instrumentation for air sampling and subsequent analysis, while being a core item of any system of air quality control, can provide for routine air sampling only at few stations, and primarily for the near-ground atmospheric layer. In this respect, lidar techniques have an obvious scientific and economic advantage by enabling remote observations of the entire atmospheric volume with high spatial and time resolution.

In this paper we concentrate on how lidar stations can be used as a part of a complex ecological monitoring of an industrial region. To demonstrate this we have taken, as an example, the city of Soligorsk, Belorussia. The work was undertaken in 1991–1995 by such Belorussian organizations as Academy of Sciences, Department of Natural Resources among others. The purpose is to give specific features of used measurement technique and lidar data analysis methods, to compare them with existing techniques, and to elaborate on a computer program to control air quality over industrial region.

2. THE SOURCES OF AIR POLLUTION IN SOLIGORSK INDUSTRIAL ZONE

The Soligorsk industrial zone lies in the southern part of Minsk region. Its center is Soligorsk city (52 thousand population) located on the right bank of the Sluch' river, 140 km south of Minsk. The deposits of

potassium salts (about 3.75 billion tons reserve) at the depths of 300–800 m make up the basis of its industrial potential. Four plants yield over 5 million tons of fertilizers yearly as calculated to 100% pure nutrients produced. At the same time, those plants are the sources of atmospheric pollutants and have adverse effect on the ecology of this region. The emissions comprise different gases (nitrous and sulfuric oxides,

hydrocarbons, ammonium, etc.) and large amount of dust. Each plant contributes 800 to 1400 t/yr of dust rich in KCl and NaCl.¹ The map presented in Fig. 1 shows the location of these plants. Technologically, the whole combinat consists of an concentration factory, slag stock, and a salt dump. Each component has its individual channels to emit pollutants into the environment.

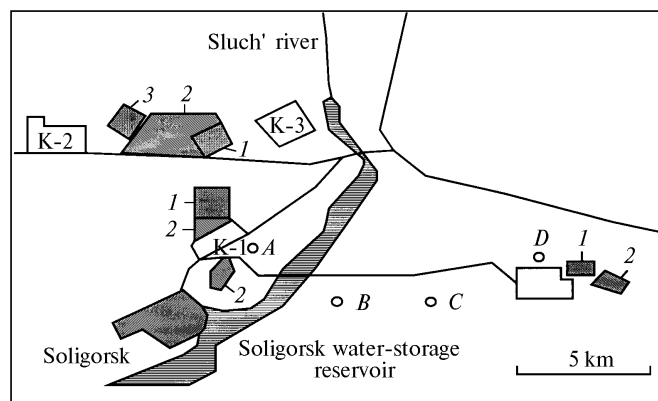


FIG. 1. Map of the Soligorsk industrial region: salt dumps (1) and slag storage ponds (2). Figures K-1, ..., K-4 denote the locations of potassium plants, and letters A, B, C, and D mark the locations of aerosol plane-table samplers.

After being lifted from the mine, the sylvinitic ore is conveyed to the concentration factory for ore crushing, floatation separation of KCl from NaCl, pressing, crushing, and granulating of the potassium fertilizers. Early in the technological cycle, the generated dust is removed through low-lying, roof-mounted pipes of the suction apparatus. The dust by-produced (mostly KCl-bearing) at the subsequent technological processing is ejected through tall (40- to 120-m height) plant stacks. The plants also comprise thermal stations and boilers, whose combustion products are released through tall stacks (60- to 120-m height).

The salt dumps having the areas of several square kilometers represent distributed sources of dust. Finely dispersed salt particles are blown out by wind high into the atmosphere. The intensity of this process is determined by the state of the atmosphere and wind velocity.

On the plant's territory and nearby there are normally performed construction, loading-unloading, and transportation work, and there are other enterprises, that also contribute to the dust loading of the atmosphere. All these processes create a spatially inhomogeneous and dynamic pattern of the pollution field over the plant region.

Besides the potassium plants, also operated in Soligorsk city and its suburbs are over fifty enterprises emitting, though much less, pollution. On the whole, the total intensity of pollution sources in Soligorsk

region is estimated to be of 530 t/(km²·yr), what is more than sufficient to classify it as an ecological crisis and ecological catastrophe zone.¹

3. LIDAR MONITORING OF ATMOSPHERIC PARAMETERS AT ECOLOGICAL SURVEY OF AN INDUSTRIAL CENTER

Lidar measurements as a part of the complex ecological survey have been used to determine the level of air pollution by dust, to identify dust sources, estimating their strengths, mapping the dust mass concentration, and evaluating the rate of dust sedimentation. Simultaneously with lidar measurements, chemical and size-spectrum analyses and beta-activity measurements of dust samples were carried out to deduce aerosol concentration and composition. Meteorological parameters of the atmosphere have also been measured during a survey.

In view of a complicated structure of the pollution sources in the industrial region and the variability of aerosol parameters due to changing level of technological activity at the enterprises and varying meteorological situations, an exorbitant number of experiments are required there to describe the processes of the aerosol field transformation. To minimize the cost and duration of experiments, we confined ourselves to field measurements of source strengths for major pollutants only and to drawing maps of aerosol concentration for a few typical zones of the industrial

region. In terms of the information accumulated, a computer code was developed to model transport of aerosol pollutants in the region under study, its input parameters being the pollution source strengths and meteorological quantities measured. The aerosol concentration calculations were compared with observations.

4. INSTRUMENTATION AND METHODS FOR RETRIEVING ATMOSPHERIC AEROSOL PARAMETERS FROM LASER SENSING DATA

We used a mobile lidar station (MLS) to study the dynamics of spatial distribution of the atmospheric aerosol concentration over the industrial region. The MLS is a multi-purpose lidar mounted in an automobile van. Inside the van there is a closed part with two working places for operators equipped with a host computer, multichannel data recording system, control system over station's drives and working mechanisms, and other instruments.

The receiving-transmitting system of the lidar is mounted on a rotatable platform that may be lifted from inside the second module of the van. Depending on the instrumentation used, the radiation at working wavelengths of 694 or 532 and 1064 nm is used. The MLS six-channel receiving optical system enables the multi-wavelength sensing in an analog or photon-counting mode. The station also provides for measuring the depolarization of return signals.

A portion of data on the spatial distribution of the aerosol concentration was acquired with a multispectral Gloria M lidar operating at 7 wavelengths from 380 to 965 nm.² However, its primary function was to acquire spectra of atmospheric optical parameters for the purpose of constructing regional optical models of the atmosphere in the region under study.

The algorithm of laser sensing data processing was tuned to measure the mass concentration of atmospheric aerosol. Some measurements have been carried out as a single-wavelength sensing of the atmosphere at either 532 or 694 nm wavelength, while other were essentially multispectral with the number of working wavelengths ranging from 2 to 7. Regardless of the version used, the processing procedure involved, as an intermediate step, calculation of the aerosol backscattering coefficient β at a reference wavelength (either 532 or 694 nm). It was those wavelengths for which the ratio of aerosol backscattering coefficient to the aerosol mass concentration was determined to calibrate the lidar.

The algorithm of β calculation is based upon the solution of the system of lidar equations which relate the intensity of return signals $P(\lambda_i, l)$, at the wavelength λ from a region at a range l along the sounding path, to the atmospheric optical parameters

$$P(\lambda_i, l) = A(\lambda_i, l) P_0(\lambda_i) l^{-2} \beta(\lambda_i, l) \times$$

$$\times \exp \left\{ -2 \int_0^l \varepsilon(\lambda_i, l') dl' \right\}. \quad (1)$$

Here $\beta(\lambda_i, l)$ and $\varepsilon(\lambda_i, l)$, $i = 1, \dots, n$, are the aerosol backscattering and extinction coefficients, n is the number of working wavelengths, $A(\lambda_i, l)$ is the instrumental constant, and $P_0(\lambda_i)$ is the energy of a sounding pulse. The optical characteristics $\beta(\lambda_i, l)$ and $\varepsilon(\lambda_i, l)$ are two-component values

$$\beta(\lambda_i, l) = \beta_a(\lambda_i, l) + \beta_m(\lambda_i, l); \quad (2)$$

$$\varepsilon(\lambda_i, l) = \varepsilon_a(\lambda_i, l) + \varepsilon_m(\lambda_i, l). \quad (3)$$

Here symbols a and m stand for the aerosol and molecular components, respectively. Values of $\beta_m(\lambda_i, l)$ and $\varepsilon_m(\lambda_i, l)$ are calculated from data of meteorological measurements. To provide a closure for the equation set (1)–(3), extra equations relating $\beta_a(\lambda_i, l)$ to $\varepsilon_a(\lambda_i, l)$ are required. Here, we use the method of optimal linear estimation,³ in which the aerosol extinction coefficient is represented as a linear form

$$\varepsilon_a(\lambda_i) = \sum_{j=1}^n c_{i,j} \beta_a(\lambda_j). \quad (4)$$

The coefficients $c_{i,j}$ were evaluated using *a priori* information on the aerosol studied following the algorithm from Ref. 4. For the case of single-wavelength sensing, the method is essentially identical to that of *a priori* presetting the lidar ratio for the atmospheric aerosol particles. When switching to multispectral sensing, the set of parameters $\beta_a(\lambda_i, l)$ is sufficient to construct relations of the type (4), thereby allowing $\varepsilon_a(\lambda_i, l)$ to be evaluated reasonably accurately given rather broad assumptions on aerosol particle microstructure. For instance, the error is 15% when $C = 7$ (see Ref. 5).

The system of equations (1)–(4) was solved following the algorithm from Ref. 6. The calculated $\beta_a(\lambda_i, l)$ values for a reference wavelength, 532 or 694 nm, were used to evaluate the aerosol mass concentration M from a simple relation

$$M = \mu(\lambda_i) \beta_a(\lambda_i). \quad (5)$$

As is commonly accepted, we have evaluated the parameter μ from calibration measurements when sampling aerosol near the sounding path. The samples collected were then separated into fractions and weighed fraction-by-fraction. Using this method, the mass concentration is estimated accurate to approximately 0.1 mg/m³, provided the samplings are not too far separated in time.⁸ For the 694 nm wavelength the average μ value is 20 $\mu\text{g}\cdot\text{km}\cdot\text{sr}/\text{m}^3$, standard deviation being about 60%. The parameter μ is known to widely vary, depending on the aerosol type

and air humidity.⁹⁻¹¹ For these reasons, we always tried to make measurements of aerosol spatial distribution in parallel to calibrations. Indeed, the uncertainty of M determination was within the error of calibration measurements for a homogeneous aerosol field, and it usually grew due to the scatter of μ values within the above limits when aerosol microstructure changed.

No less important task of the experimental work was to study the aerosol particle fluxes in the atmosphere. To estimate aerosol fluxes through a certain boundary, the wind field information is required besides the spatial distribution of aerosol mass concentration. In our calculations, we took the wind field to be horizontally uniform, while vertically, the wind velocity distribution was modeled empirically as discussed in Refs. 12-14 (to be shown in section 6 below). Meteorological measurements from the stations were used as model input, as well as wind velocity measurements acquired just near the lidar station at about 10-m height. When possible, we have also used higher objects available within the region under study to measure wind velocity at higher levels. Normally we made measurements in the evening, when the atmospheric stratification was indifferent or weakly stable.

5. EXPERIMENTAL STUDIES OF AEROSOL FIELDS IN THE INDUSTRIAL ZONE

The lidar stations were used to measure distributions of mass concentration of aerosol pollutants over all four potassium plants under study. Figure 2 presents the scheme of aerosol soundings in the region of the Kalii 2 plant. Set out in the figure is the territory of the concentration plant, with marks indicating the locations of the tall stacks of the plant through which dust is removed from different technological installations. Lidar data, representing an array of horizontal (over azimuth angle) and vertical (over zenith angle) scans, show the spatial distribution of aerosol mass concentration $M(r)$ over the plant region. A total of 2 to 4 experiments were performed, each being of 3-6 h duration. The experimental results were then processed to map the distributions of aerosol mass concentration M over the vertical and horizontal transects. The maps of dust distribution over the horizontal transects were then used to identify zones where the atmospheric pollution exceeded the maximum permissible level. The M distributions over vertical transects, whose traces on the horizontal plane are shown in Fig. 2a by dashed lines numbered 1 through 6, together with wind velocity measurements in the near-ground layer were used as input to estimate aerosol particle fluxes in the atmosphere and pollution source strengths. Atmospheric pollution by the other plants under study was sensed using the same measurement scheme.

Pollution of the atmosphere over regions of potassium plants was studied, and the results were mapped as spatial distributions of dust mass concentration over horizontal transects at heights of 10-15 m (see Fig. 2). These measurement data presented are averaged over 3-6 h, so the short-term variations of aerosol fields due to changing intensity of aerosol emissions and wind velocity are smoothed. The mapped distributions of the aerosol mass concentration were plotted for the four plants and surroundings. From 1992 to 1994 a series of measurements was carried out for different levels of technological activity and various production facilities operated. From analysis of the experimental material it can be concluded that at the distances of 2-3 km in the downwind directions, there exist zones where pollution values are constantly in excess of daily average maximum permissible concentrations of $0.15 \mu\text{g}/\text{m}^3$ (see Ref. 8). The measurements have allowed us to outline the contaminated zones and estimate the level of their contamination.

Inspection of maps of aerosol concentration has revealed zones whose pollution source was hard to identify. Possibly, this is due to a significant secondary wind lifting of dust settling down in the industrial zone of the plant. Importance of this mechanism of dust formation was hypothesized in Ref. 3 based on analysis of changes in the ratios of ion (K, Na, and Cl) dust composition.

The intensity of aerosol emissions was estimated from the distributions of aerosol over vertical cross sections. The vertical planes in which the distribution of aerosol mass concentration was measured have been set by the azimuth directions that are optimal, regarding the spatial resolution and position of the pollution sources, for the territory of each plant.

Maps of horizontal cross sections for potassium plants 2 and 4 are shown in Fig. 2, with traces of vertical planes shown by dashed lines. Figures at the dashed lines are the numbers of vertical cross sections. Figure 3 presents the contours of aerosol distribution over vertical planes. The family of the concentric contours (Fig. 3b) portrays the dust release from the tall plant stack. Change in aerosol distribution pattern between transects 3 and 6 is due to an increase in the number of pollution sources acting when going from windward to leeward side of the plant territory. For a series of measurements, we have constructed a model of vertical distribution of wind velocity (to be described in section 6) and evaluated the aerosol particle fluxes through fixed planes. Intensities of pollution sources located between the fixed planes were found by taking difference of fluxes through the corresponding transects. Finally, we have estimated the dust source intensities, both for the plant as a whole and its separate objects.

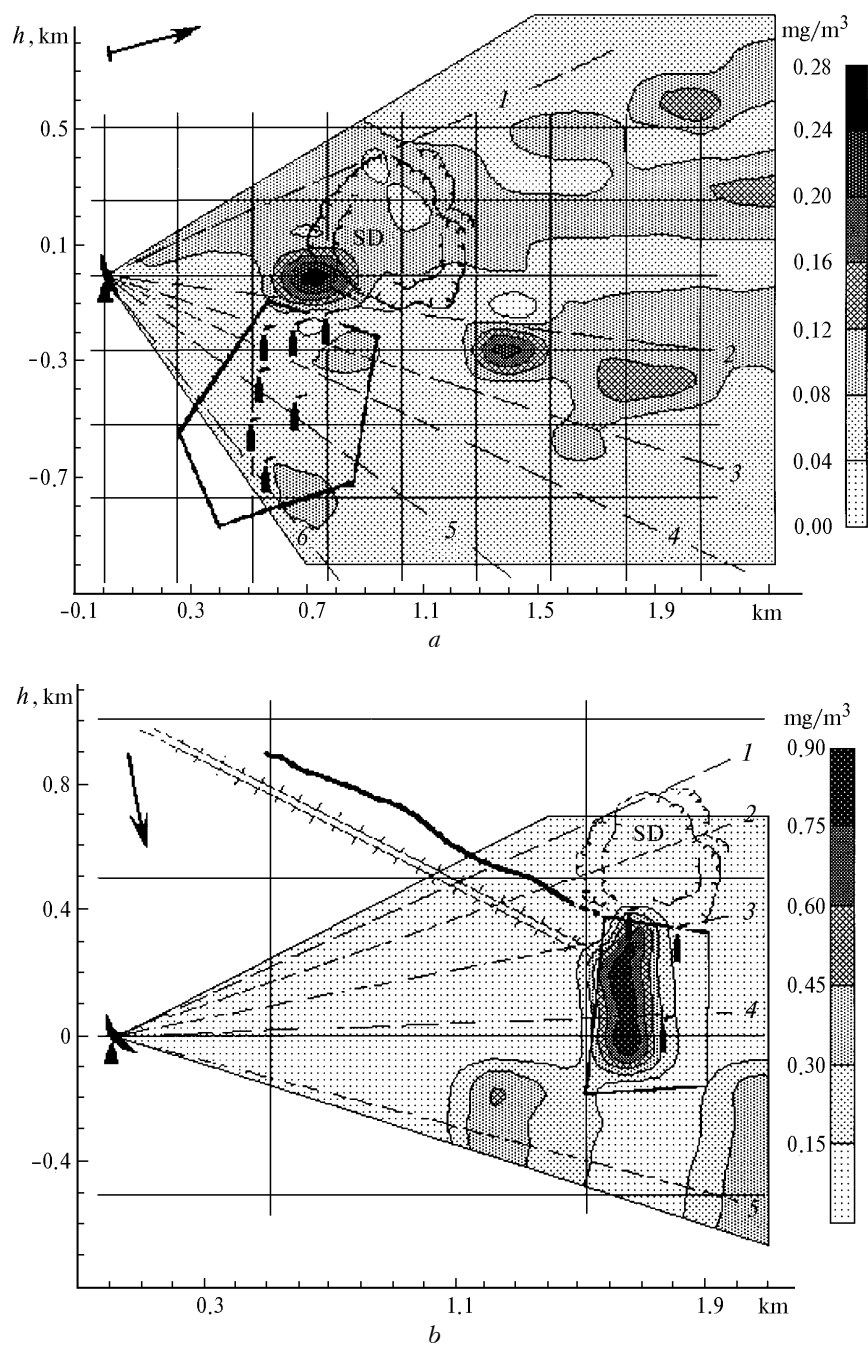


FIG. 2. Distribution of aerosol mass concentration in the potassium plant regions (horizontal transects): (a) Kalii 2 on July 9, 1993, and (b) Kalii 4 on July 5, 1993. Arrow indicates wind direction. The abbreviation SD shows locations of salt dumps. Numbers (1 to 6) at lines are traces of vertical cross sections.

It should be noted that thus detailed measurements of aerosol field transformation were only possible on days with low technological activity, and impossible on the other days when an optically dense plume interfered the lidar measurements. Also there may occur changes in aerosol microstructure after releases from stacks as noted in Ref. 10.

Table I presents estimates of the total intensity of dust emissions from the potassium plants, obtained using the above technique. The calculated values of maximum permissible emissions, with the account for specific features of the technological processes and their nominal activity level, are given in column 5 of the Table I. At the time of measurements, in summer and

fall of 1993, the technological activity was minimal for these plants, with accordingly low emission intensities measured in the experiment. Repeating the same lidar measurements in about one hour interval gave appreciably different results by approximately 15–30%. Gradual decrease in the intensity of emissions from Kalii 1 plant is due to stepped-down switching off of the technological installations. The event of extremely high intensity of the emission from Kalii 2 plant at 22:00 LT on July 8, 1993, is likely to be associated with the break of technological process regulations at the plant.

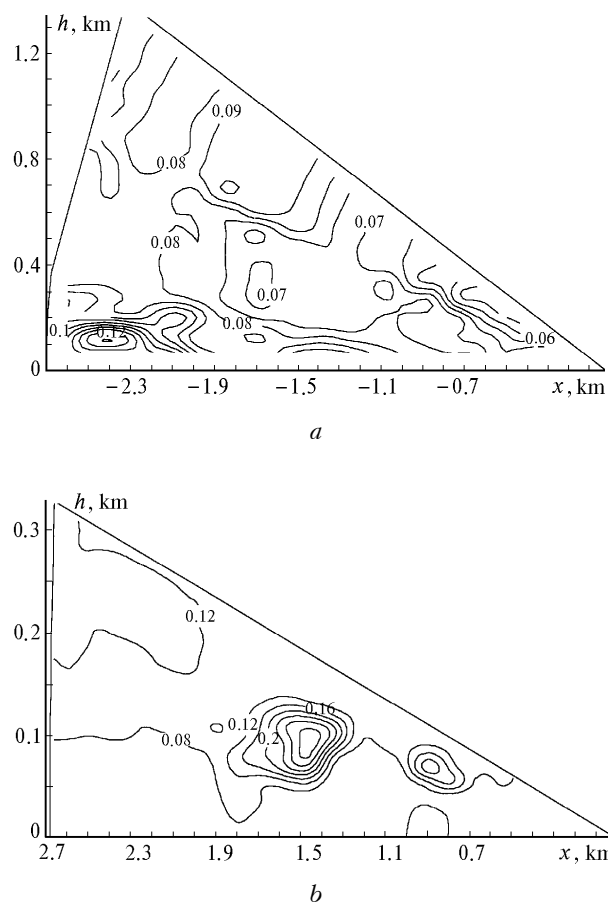


FIG. 3. Distribution of aerosol mass concentration in the Kalii 2 plant region on July 7, 1993: (a) transect 3 and (b) transect 6.

It was of special interest to estimate the intensity of aerosol blowing out from the waste rocks for determining its role as a channel of salting the environment. As lidar measurements showed, at low wind speeds no significant increase in the aerosol concentration was observed over the dump territory. However, since each dump may occupy the area of up to several square kilometers together they may produce a significant contribution. The intensity of dust blowing out from rocks was studied in the laboratory as a function of the rock's state parameters and air blow speed.¹⁴ However, large errors may occur in the

estimate of the intensity of such an emission source because its actual parameters were known only approximately.

TABLE I. Emission rates of potassium plants.

Plant	Date of measurement	Start/end time of measurement	Emission rate, t/yr	Emission rate (maximum permissible value), t/yr
Kalii 1	24.06.93	21:40/23:10	662	1327
	28.06.93	22:30/24:00	508	–
	29.06.93	21:55/23:57	315	–
	30.06.93	21:34/23:40	243	–
	01.07.93	22:10/23:30	79	–
Kalii 2	08.07.93	20:47/21:15	950	1443
	09.07.93	21:20/22:36	4813	–
Kalii 3	01.10.93	17:30/20:00	81	1043
	05.07.93	22:12/23:59	662	785
Kalii 4	07.07.93	20:40/23:30	465	–

Lidar measurements of the intensity of aerosol blowing out from the rock dumps were performed for the region of Kalii 4 plant, which is well far from the town and other localized pollution sources and so their distorting effect on results is minimal. The measurements were taken on July 5, 1993. The wind blew from the rock dumps toward the plant (Fig. 2a) at a speed of 2 to 3 m/s. Aerosol distribution was analyzed in the volume bounded by transects 1 and 2, i.e., over half of the area of the dumps. Based on the flux difference estimate, they were found to contribute 6% to the total aerosol emissions from the plant.

6. MATHEMATICAL SIMULATION OF THE AEROSOL TRANSPORT

Large amount of dust material emitted from the potassium plants to high atmospheric altitudes through the tall stacks can then be spread over a large territory and considerably affect its ecology. It is a difficult task to study spatial and temporal variations of the pollution fields in different meteorological situations. Therefore, the development of a mathematical model of the pollution transport was an important part of the integrated work on ecological monitoring of the region.

Transport of pollutants in the atmosphere occurs through their average joint drift with the medium as a whole, their turbulent diffusion, and their gravitational sink. This complex process was described based on the equation of turbulent diffusion for an admixture concentration $M(x, y, z)$, with the OX axis oriented in the downwind direction and OZ axis vertically upward. The strength of sources and surface sinks for an admixture were accounted for through the boundary

conditions. Because the cross-wind (along OY axis) aerosol distribution is primarily determined by fluctuations in wind direction, the admixture concentration can be approximately factored as

$$M(x, y, z) = p(x, y) q(x, z). \quad (6)$$

Thus we need to solve numerically a two-dimensional diffusion equation for concentration $q(x, z)$ integrated over OY axis, and multiply the result by the experimentally determined^{15,16} function $p(x, y)$ which has the meaning of the cross-wind aerosol distribution. In the near-ground atmospheric layer (NAL), up to 10–50 m altitude, the altitude dependence of wind velocity $u(z)$ and coefficient of turbulent diffusion $k(z)$ are given by the Monin-Obukhov theory¹² as

$$\frac{\partial u}{\partial z} = \frac{u^*}{\chi z} \phi(\xi), \quad k_z(z) = \frac{\chi u^* z}{\phi(\xi)}, \quad (7)$$

$$\phi = \begin{cases} 1 + \beta \xi, & \xi \geq 0 \\ (1 - \gamma \xi)^{-1/4}, & \xi \leq 0 \end{cases}, \quad \xi = z/L,$$

$$L = -\frac{TC_p \rho (u^*)^3}{\chi g H}, \quad (8)$$

where u^* is the drag coefficient; χ is the Karman's constant; ϕ is a universal constant whose approximation is given by expression (8); $\beta = 6$ and $\gamma = 16$ are constants; T and ρ are near-ground temperature and air density; C_p is the specific heat of air; H is the vertical turbulent heat flux; g is the acceleration of gravity; and L is the Monin-Obukhov length, quantitatively characterizing the degree of atmospheric stability.

To determine the wind velocity and diffusion coefficients at extra-NAL altitudes, we used universal profiles obtained by Byzova and colleagues^{16–19} based on data of several-year observations of the atmospheric meteorological parameters from a 300-meter high mast and on the results of numerical simulation of the atmospheric boundary layer (ABL) structure. The atmospheric temperature stratification, which strongly determines the altitude distributions of $u(z)$ and $k(z)$, was deduced from such meteorological quantities as cloud height and cloud fraction, visibility range and wind velocity at the weather vane altitude, as well as based on time of day and date.²⁰

Figure 4 compares lidar data with calculated particle distributions along OY and OZ axes for releases from the potassium plant stack. As the measurements show, the maximum concentration is about $2 \mu\text{g}/\text{m}^3$ at a distance of 0.5–1 km from the stack, with characteristic cross-sectional size being

nearly 100 and 20 m in the OY and OZ directions, respectively.

Also, distribution of aerosol from a point source was calculated in the cross-wind plane at a distance of 700 m from the stack.¹⁴ In this case the stack was 100 m tall, the wind velocity at the weather vane altitude was 2.8 m/s and aerosol particles were assumed to have diameter of one micron. We have also assumed that weakly stable stratification of the atmosphere, characteristic of twilight conditions, occurred. From Fig. 4 we see that calculated results agree reasonably well with the lidar data on dust distribution in the plume.

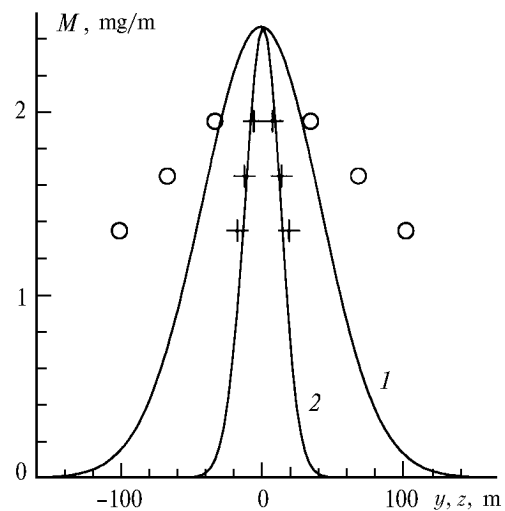


FIG. 4. Comparison of calculated and measured distributions of particle concentration in the emission jet along OX (curve 1 and marks \circ ,) and along OZ axis (curve 2 and marks $+$, respectively).

The above discussed method of calculating the dispersal of admixtures from an isolated source was used to develop a computer code for estimating and predicting the state of air basin over Soligorsk. The input parameters to the model of an admixture dispersal include meteorological data and pollution source characteristics, such as the intensity of emission from the stacks and salt (NaCl) particle fluxes from the surface of salt dumps. The intensity of emissions from the stacks was estimated using specifications of individual technological installations, information on the level of technological activity at the plants from Belarus'kalii administration, and the data of field measurements.¹³

The results of model calculations were verified against the measurements of the near-ground concentration and sedimentation rate of salt dust. The sedimentation was sampled using gauze plane tables installed along the road connecting the 1st and 4th plant. The dust concentration was measured by isokinetic probes. The locations of the sampling tables

are marked by letters *A*, *B*, *C*, and *D* on the map (Fig. 1). Individual samples were accumulated for three days, but the plane-table gauze was renewed every day. The plane-table's gauze and sampling filters have then been insulated, and ion-selective electrodes used to determine concentrations of K, Na, and Cl ions and, thereby, to evaluate the sedimentation rates and concentrations of NaCl and KCl dust aerosols.

For a comparison with the experiment, calculations were made every 3 hour (i.e., at the rate of meteorological measurements), with the subsequent averaging for 3 days. The results of comparison are presented in Table II. We estimate the agreement between calculated and measured values of K (KCl) to be quite satisfactory. The calculation-to-measurement discrepancy for the spatial distributions of NaCl concentration and sedimentation rate may be due to unknown source of NaCl dust particles, that most likely is distributed in space.

TABLE II. Calculated and measured mean sedimentation rates of K and Na ($\mu\text{mol}/\text{m}^2$ day).

Point	K		Na	
	Experiment	Calculation	Experiment	Calculation
A	5.5	10.6	116	215
B	1.6	1.3	87	10
C	1.0	0.85	109	7
D	0.86	2.8	90	191

7. CONCLUSION

Use of lidars to study the dust pollutions, formation of aerosol pollution fields, and aerosol transport and sedimentation, has enabled us to collect experimental data on the pollution source parameters and structure of aerosol fields over an industrial center, which could have been too much expensive, if at all possible, by any other means. However, it is the integrated character of studies we have performed that has allowed us to achieve the results that should be of primary use when making decisions on measures to improve ecological situation in the region. Among those there are the strengths of individual pollution sources, zones with enhanced pollution loading identified, and the role of the atmosphere estimated as a channel of agricultural soil salting.

To make lidar ecological monitoring more efficient, some methodological and technical problems have to be solved in the laser sensing method. To estimate the emission rates and to study the pollutant transport, it is important to know real distribution of wind speed and direction in the atmospheric boundary layer. This again could be done by employing laser sensing techniques, like, for example, Doppler lidar or correlation analysis technique. Another one way of increasing the potentialities of lidar techniques, in application to ecological monitoring of atmospheric aerosols, could be the use of multi-wavelength polarization lidars. In so

doing the accuracy of aerosol mass concentration estimation may be improved, its classification performed, and applicability of lidar methods could be extended to the case of optically dense aerosol layers, because of the possibility of correcting lidar returns for multiple light scattering.

REFERENCES

1. A.V. Matveev, A.A. Lishtvan, A.A. Kovalev, et al., "Ecological-radiative characterization of administrative region (by example of the Soligorsk region), B Preprint No. 25, Ekomir Republic Scientific-Technical Center of Remote Sensing of Environment, Minsk (1994), 76 pp.
2. A.N. Borodavka, E.M. Gitlin, V.I. Gubskii, et al., *Catalogue of Instrumentation* (Nauka i Tekhnika, Minsk, 1988), pp. 28–29.
3. A.P. Chaikovsky, V.N. Shcherbakov, and S.B. Tauroginskaya, in: *Abstracts of Papers at the 17th International Laser Radar Conference*, Japan (1994), pp. 18–19.
4. S.B. Tauroginskaya, A.P. Chaikovsky, and V.N. Shcherbakov, *Atmos. Oceanic Opt.* **7**, No. 10, 753–757 (1994).
5. A.P. Ivanov, A.P. Chaikovskii, F.P. Osipenko, et al., *Izv. Akad. Nauk, Fiz. Atmos. Okeana* **30**, No. 3, 411–416 (1994).
6. B. Mil'ke and V.N. Shcherbakov, *Atm. Opt.* **4**, No. 3, 248–251 (1991).
7. *Guidelines on Atmospheric Pollution Monitoring, Document 5402 186–89* (Goskomgidromet SSSR-Minzdrav SSSR, Moscow, 1991).
8. V.P. Andryukov and I.B. Pudovkina, *Meteorol. Gidrol.*, No. 1, 101–107 (1993).
9. V.E. Zuev, B.V. Kaul', I.V. Samokhvalov, et al., *Laser Sensing of Industrial Aerosols* (Nauka, Novosibirsk, 1986), 188 pp.
10. G.G. Matvienko, *Atmos. Oceanic Opt.* **8**, No. 1–2, 125–136 (1995).
11. Yu.S. Balin and I.A. Razenkov, *Atmos. Oceanic Opt.* **6**, No. 2, 104–114 (1993).
12. A.S. Monin and A.M. Yaglom, *Statistical Hydromechanics* (Nauka, Moscow, 1965), Vol. 1, 639 pp.
13. I.A. Bril', M.A. Drugachenok, V.P. Kabashnikov, et al., "Study of wind transport of salt dust in Soligorsk industrial region, B Preprint No. 12, Ekomir Republican Scientific-Technical Center of Remote Sensing of Environment, Minsk (1993), 50 pp.
14. A.I. Bril', V.P. Kabashnikov, A.A. Kovalev, et al., "Development of mathematical model of sources, dispersion, and sedimentation of aerosol and gaseous admixtures in the air basin of Soligorsk industrial region, B Preprint No. 20, Ekomir Republic Scientific-Technical Center of Remote Sensing of Environment, No. 20, Minsk (1994), 56 pp.
15. M.E. Berlyand, *Current Problems in Atmospheric Diffusion and Pollution* (Gidrometeizdat, Leningrad, 1975), 448 pp.

16. N.L. Byzova, V.N. Ivanov, and E.K. Garger, *Turbulence in the Atmospheric Boundary Layer* (Gidrometeoizdat, Leningrad, 1989), 341 pp.
17. N.L. Byzova, V.L. Shnaidman, and V.N. Bondarenko, *Meteorol. Gidrol.*, No. 11, 75–83 (1988).
18. N.L. Byzova, ed., *Typical Characteristics of the Lower, 300-m thick Atmospheric Layer from High Mast Measurements*, (Gidrometeoizdat, Moscow, 1982), 67 pp.
19. N.L. Byzova and L.K. Kulizhnikova, *Meteorol. Gidrol.*, No. 5, 60–69 (1996).
20. *Atmosphere, Handbook* (Gidrometeoizdat, Leningrad, 1991), 508 pp.